



PERGAMON

Applied Thermal Engineering 19 (1999) 543–554

---

---

APPLIED THERMAL  
ENGINEERING

---

---

# Temperature measurement in the swirl chamber of an IDI engine using Moire deflectometry

D.T. Li<sup>a</sup>, R. Xiong<sup>a</sup>, H. Xue<sup>b,\*</sup>

<sup>a</sup>*Department of Power Engineering, Jiangsu University of Science & Technology, Zhengjiang, 212003, People's Republic of China*

<sup>b</sup>*Department of Mechanical & Production Engineering, National University of Singapore, 10 Kent Ridge Crescent, Singapore, 119260*

Received 1 May 1997

---

## Abstract

The processes of ignition and combustion of a diesel engine are affected by temperature distribution formed during compression stroke. We present an applied study on the measurement of temperature distribution in the swirl chamber of an IDI engine using the Moire deflection technique. The method for determining the quantitative temperature distribution from detected Moire fringe shift has been established. From the measured temperature distribution, the evaporation and air mixing processes in the swirl chamber during compression stroke is analysed and discussed. The temperatures mapped by Moire deflectometry are compared and validated with the temperatures measured by hot-wire anemometry at several representative points. The experimental investigation opens up a new means for measuring the temperature distribution in the combustion chamber of IC engines. © 1998 Elsevier Science Ltd. All rights reserved.

*Keywords:* IC engine; Swirl chamber; Temperature measurement; Moire deflectometry

---

## 1. Nomenclature

$h$	deviation of Moire fringe
$l$	length of the objective flow field along the transmitting direction of the light
$n$	refractive index
$r$	cylindrical co-ordinate, $r = \sqrt{x^2 + y^2}$
$T$	temperature

---

\* Corresponding author.

$x, y, z$	Cartesian co-ordinates as defined in Fig. 1
$y^+$	non-dimensional distance from wall
$\Delta$	distance between two gratings
$\alpha$	deflection angle
$\theta$	rotating angle of two gratings
$\lambda$	wavelength of light
$\varphi$	crank angle
<i>Subscript</i>	
0	reference point

## 2. Introduction

Measurement of temperature distribution in the combustion chamber of an IC engine is extremely important for understanding the combustion process of the engine. However, difficulties come from various aspects such as constrained structure, high temperature and high pressure in the chamber, and instability of the process. Over the years, contact measurements have been the dominant means to determine the temperature field [1], but the results of these methods are not satisfactory. The thermal inertia of contact sensor and the interference with measured flow field constantly affect accuracy and certainty of the measurement. On the other hand, when the non-contact optical method is used to measure the temperature distribution, the deflection effect of the light beam in the temperature field is usually neglected. Vest [2] suggested using an imagery lens for the correction of the deflection, but the process was rather tedious. In 1980, Kafri [3] proposed for the first time that Moire deflectometry could be used for transient temperature measurement. Afterwards, Keren [4] used the method to measure one-dimensional (1D) temperature distribution of an axisymmetric steady flame. Recently, Almanasreh and Abushagur [5] used Moire deflectometry to measure the density distribution of a candle flame as a phase object. Toker et al. [6] indicated that Moire deflectometry yielded a more accurate measurement of the temperature and density distribution in complex compressive flow fields, compared with Schlieren and shadowgraphy.

Moire deflectometry has a simple optical system, a moderate requirement on coherency of the light source, and is easy for operation. When it is used for measurement of an axisymmetric temperature field, mathematical formation is straightforward. As a result of these advantages, we are motivated to apply the Moire deflectometry to the swirl chamber of an IDI engine. In spite of the success by Stricker et al. [7–9], who measured the distribution of density and temperature in the jet ejecting field of a rocket engine, the high temperature, high flow speed, and high pressure environment in the swirl chamber, set up many barriers for the application. The geometric constraints of the swirl chamber prevent observers from obtaining sufficient Moire deflection patterns at different directions. Furthermore, in the swirl chamber, there is no surrounding area which can be used as a reference point to determine temperature quantitatively.

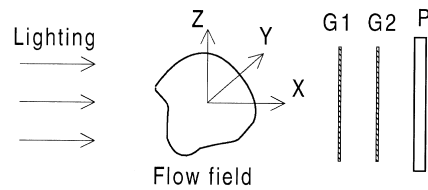
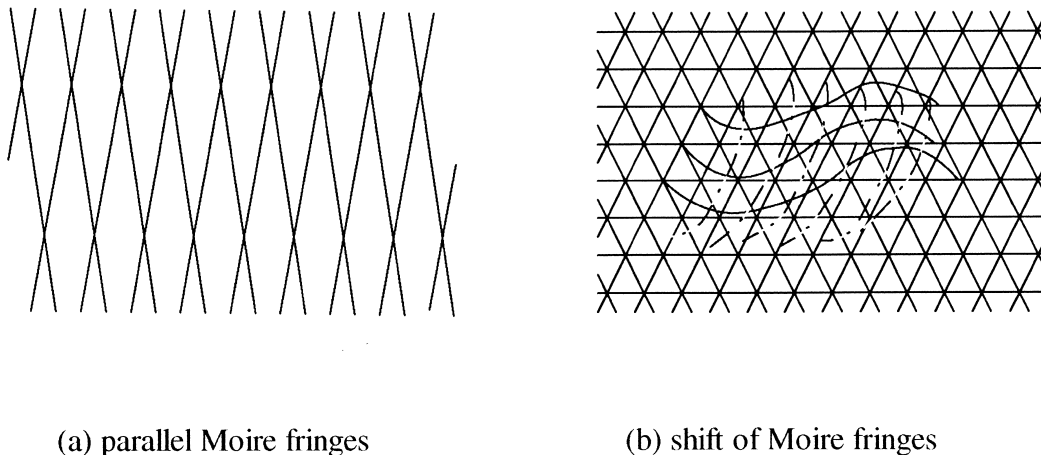


Fig. 1. Schematic of a simple Moire deflectometry.

In this work, we developed a new method to measure the transient temperature distribution using Moire deflectometry in a swirl chamber of an IDI engine. The results of the measurement are validated by a hot-wire anemometry. Satisfactory results have been achieved. Possible improvements for design of the fuel evaporation and mixing processes in combustion chambers of IDI engines are suggested.

### 3. Principle

According to the Fermat principle, when a beam of light passes through a flow field, the change in the index of fluid refraction will produce a deflection effect on the light beam. The deflection effect is exactly employed by Moire deflectometry to measure the refractive index. Fig. 1 is a schematic of a simple Moire deflectometry. A sheet of light passes through an objective flow field, enters a pair of gratings G1 and G2, which are tilted with an angle  $+\theta/2$  and  $-\theta/2$  relative to the  $z$  axis, and finally reaches a receiving screen P where overlapped Moire fringes can be detected. As shown in Fig. 2, if the refractive index of the flow medium is uniform, a straight and unperturbed Moire pattern is obtained. In cases where changes of temperature and density distribution in the field occur, that is, the presence of a phase object



(a) parallel Moire fringes

(b) shift of Moire fringes

Fig. 2. Patterns of Moire fringes.

with a gradient of refractive index, Moire fringes are then distorted on the receiving screen. The deflection can be determined carefully from the shift of the fringes.

If the objective flow field is axisymmetric, the deflection of the light can be easily related to the refractive index, which is a function of the location  $r$  in the cylindrical co-ordinate system shown in Fig. 3, by the following equation:

$$h(y) = \frac{1}{\lambda_0} \int_0^l [n(r) - n_0] dx, \quad (1)$$

where  $l$  is the length of the objective flow field along the transmitting direction of the light,  $\lambda_0$  is the wavelength of the light,  $n(r)$  is the refractive index, and  $n_0$  is the reference index.

Applying an Abel transform to the above equation, we obtain:

$$n(r) - n_0 = \frac{\lambda_0}{\pi} \int_r^{r_0} \frac{dh(y)/dy}{\sqrt{y^2 - r^2}} dy. \quad (2)$$

From Eq. (2), the distribution of the refractive index can be determined once a reference index of medium refraction is chosen. For a laser light with a wavelength of 632.8 nm, assuming the medium in the measured flow field is an ideal gas, the relationship between the local refractive index and the temperature can be expressed precisely as [8]:

$$n - 1 = \frac{0.292015 \times 10^{-3}}{1 + 0.368184 \times 10^{-2} T}, \quad (3)$$

where  $T$  is the local temperature ( $^{\circ}\text{C}$ ).

Compared with shearing interferometry, Moire deflectometry provides an exact measure of the deflection angle and is much more flexible in terms of sensitivity. These are of immediate concerns of measurement in studying the combustion process of IC engines and related areas.

#### 4. Temperature measurement

The temperature measurements using Moire deflectometry were carried out in the swirl chamber of an IDI testing engine. The main specification of the testing engine is listed in Table 1. The shape of the swirl chamber looks like a bell, as shown in Fig. 4. Circular viewing windows with a diameter of 30 mm were opened on both sides of the swirl chamber. The size

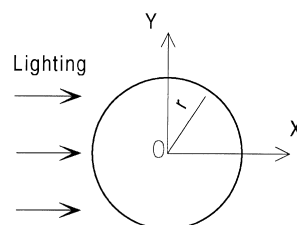


Fig. 3. A sheet of light passing through an axisymmetry flow field.

Table 1. Main specification of the testing engine

Type of engine	S195
Bore × stroke	95 × 110 mm
Volume of swirl chamber	25.7 cm <sup>3</sup>
Displacement	850 cm <sup>3</sup>
Compression ratio	19.2

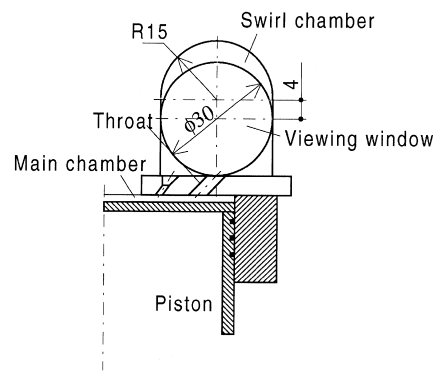


Fig. 4. Combustion chambers of the testing IDI engine.

of the window covers over 80% of the cross-sectional area to provide a comprehensive observation and measurement in the swirl chamber. The dimension of the window is carefully designed so that the opening of the window would not alter the original volume of the swirl chamber, so as to keep the compression ratio unchanged as the prototype engine. The viewing window is made of quartz, and the roughness of the surface is kept at less than 1/10 of the wavelength of the laser light, which is 632.8 nm in the He–Ne laser used in the experiments, in order to eliminate the Newton interference ring formed during measurement. The included angle between two quartz windows is precisely adjusted within a range of 10–20° to dispel the effect of the quartz background stripe on Moire fringes.

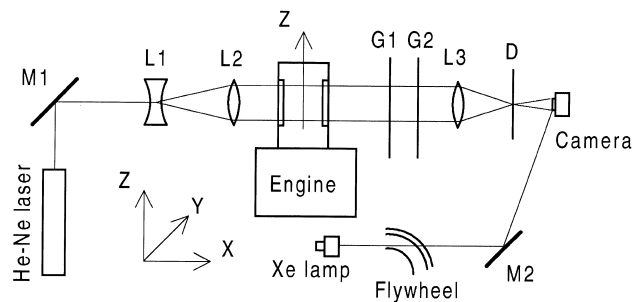


Fig. 5. Schematic of the experimental set-up.

Fig. 5 shows the Moire deflectometry system. A 50 mW He–Ne laser is used as the lighting source. The laser beam passes mirror M1 and lenses L1 and L2 to form a light sheet shining through the two quartz windows on the swirl chamber of the testing engine. When the light sheet passes through a pair of Ronchi gratings (20 lines/mm, or grating constant  $d = 0.05$ ), which are tilted with an angle  $\theta$ , Moire fringes are formed on the lens L3. The focusing lens L3 transmits the Moire deflection strips in  $+1$  (or  $-1$ ) grade to the negative of a high-speed camera, after passing through a flitting hole D. The corresponding crank angles are recorded simultaneously by the high-speed camera.

Based on the principle of the Moire deflectometry and the coordinate system shown in Fig. 5, the deflection angle is related to the refractive index by:

$$\alpha = \frac{1}{n_0} \int_0^{x_0} \frac{\partial n}{\partial y} dx. \quad (4)$$

The deflection angle may also be expressed as:

$$\alpha = \frac{h\theta}{\Delta}, \quad (5)$$

where  $\Delta$  is the distance between the two gratings and  $h$  is fringe deviation.

Since the bell-shape swirl chamber has an axisymmetric structure. It is reasonable to assume that the flow field is also approximately in axisymmetry. Thus, Eq. (4) becomes:

$$\alpha(y, z) = 2y \int_y^{r_0} \frac{\partial n(r, z)}{\partial r} \frac{1}{\sqrt{r^2 - y^2}} dr. \quad (6)$$

Applying Abel transformation and considering Eq. (5), Eq. (6) becomes:

$$n(y, z) = n_0 - \frac{\theta}{2\pi\Delta} \int_y^{r_0} \frac{h(r, z)}{\sqrt{r^2 - y^2}} dr. \quad (7)$$

Provided that the reference index of refraction  $n_0$  and the fringe deviation  $h(r, z)$  are known, the refractive index can be easily obtained by Eq. (7). As a result, temperature field can be mapped by Eq. (3).

The reference index of refraction is usually determined under atmospheric conditions such as Lian and Trolinger [9, 10], who measured the exhaust jet field of a rocket engine. However, such atmospheric reference field does not exist in the swirl chamber of IDI engines. In a confined combustion chamber, according to our experience, the temperature distribution in the turbulence viscous sub-layer ( $y^+ < 5$ ) at the near wall region is relatively stable and uniform. Therefore, the temperature at the turbulence viscous sub-layer is taken as the reference temperature and is measured simultaneously by a surface thermocouple attached to the wall surface.

The experiments were carried out in pure compression condition while the engine speed was set at 240 r/min. The engine throttle was cut off to keep the quartz window free of injection fuel and improve the quality of the Moire fringe recording. The evolution of the Moire fringe during the entire compression stroke was recorded by the high-speed camera at a speed of 1150 frames per second.

## 5. Results and discussion

Fig. 6 shows a series of Moire fringe photos at four representative crank angles during a compression stroke. The deviations of Moire stripes were read by overlapping two Moire fringe negatives. One negative of Moire fringes, which was taken before operating the testing engine, was overlapped on the objective negative of a distorted Moire deflection picture. The deviations on the overlapped pictures were then precisely determined by a special reading instrument. The data of deviation were fit to a polynomial of order 3 using the least-square algorithm. The distribution of the refractive index in the swirl chamber was obtained by

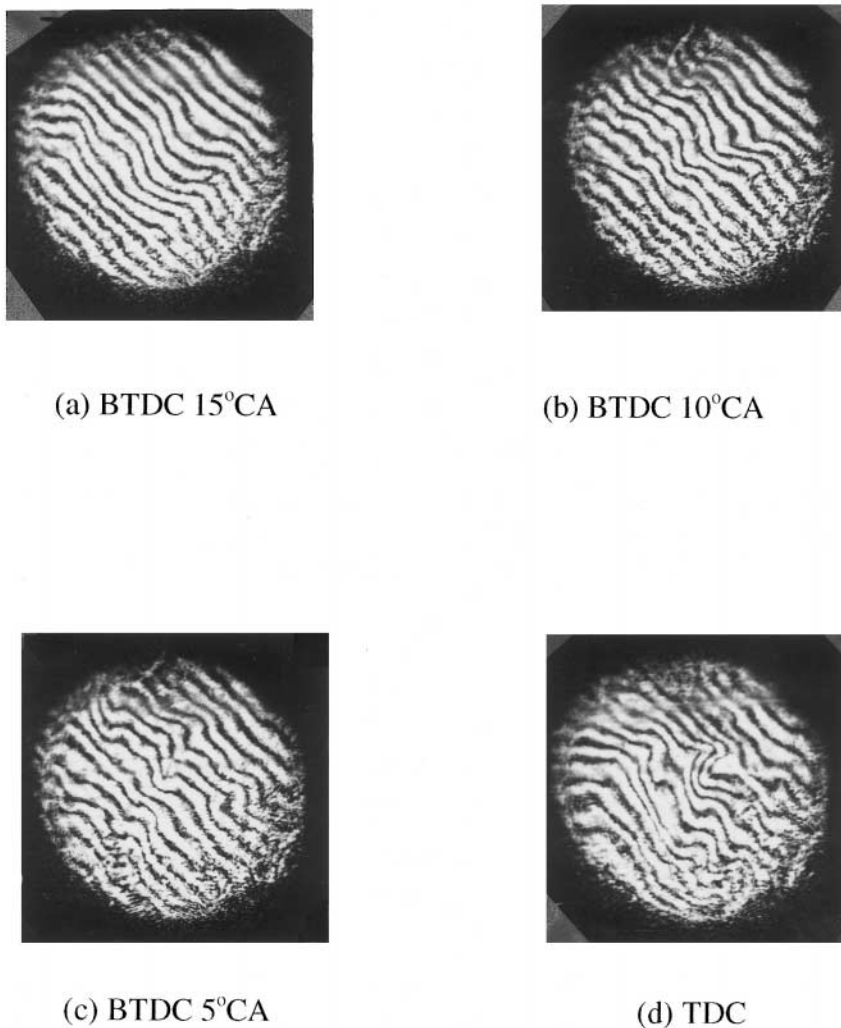


Fig. 6. Moire fringe photos at different crank angles (a) BTDC 15°CA; (b) BTDC 10°CA; (c) BTDC 5°CA; and (d) TDC.

integrating Eq. (7). Finally, the temperature mapping were obtained from Eq. (3), as shown in Fig. 7.

It is found that the gas temperatures at the central region of the swirl chamber are higher than those at the near-wall region during a compression stroke, as a result of the cooling effect

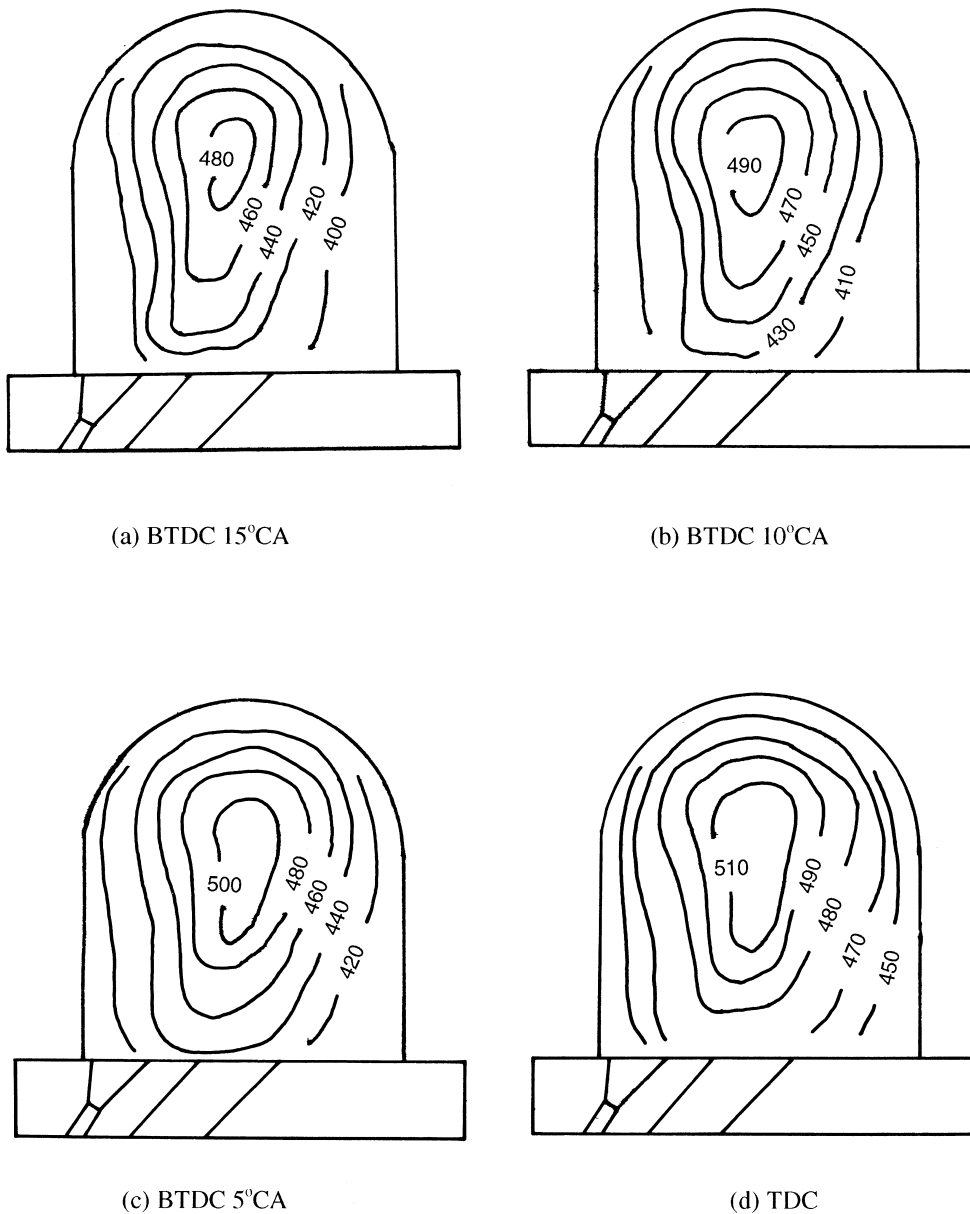


Fig. 7. Temperature distribution in the swirl chamber (a) BTDC 15°CA; (b) BTDC 10°CA; (c) BTDC 5°CA; and (d) TDC.

of the walls. With the progress of the compression stroke, the total temperature of the swirl chamber rises and the high temperature area at the up-central region gradually shifts down. There is a significant temperature difference between the left and right sides of the swirl chamber. However, the difference is getting smaller as the piston is close to TDC.

The above results imply that at the end of the intake stroke, cool and fresh air is not able to enter the swirl chamber because of structural constraints. Before a compression stroke takes place, the swirl chamber is filled with exhaust gases left over from the last cycle, and is continuously heated by the high temperature walls of the chamber. This results in the significant temperature difference between the main and swirl chambers at the early and middle stage of compression stroke. Cool air in the main chamber is initially ejected into the upright region of the swirl chamber through the inclined throat connecting the main combustion chamber and swirl chamber, as indicated in Fig. 4. Consequently, the temperature at the right side of the swirl chamber tends to be lower than that at the left. Another effect of this jet flow is that, when it impinges on the top of the chamber wall, it creates a non-uniform pressure field in the swirl chamber, that is, pressure is higher at the upper central region and is lower at the lower central region. However, the strength of the jet flow retards as the piston moves close to TDC, because the pressure difference between the main and swirl chamber decreases. This explains the reason why the high temperature region shifts down during the compression stroke.

From Fig. 7, it is obvious that the high temperature region is located at the central area of the swirl chamber at the late stage of the compression stroke. Therefore, the angle of engine injection can be optimized to allow most of the injected fuel to pass through the central region. The effect might be twofold. Promoting the evaporation and mixing of the fuel is definitely desirable. Injecting part of the fuel directly into the main combustion chamber after passing through the high temperature central region is again very important, since the combustion can be followed through the heat release model of DI engines.

In order to validate the temperature measured by Moire deflectometry, five representative temperature points were selected and measured by a hot-wire anemometry. The positions

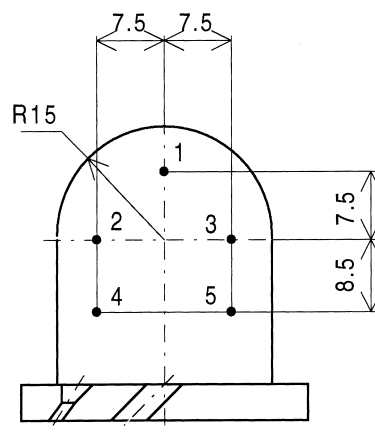


Fig. 8. Measurement points for hot-wire anemometry.

measured by the hot-wire anemometry are indicated in Fig. 8. The results are compared with the temperature mapped from Moire fringes at the five different locations over a complete compression stroke, as shown in Fig. 9. The results show that the measured temperatures by hot-wire anemometry at all five points are slightly lower than that by Moire deflectometry.

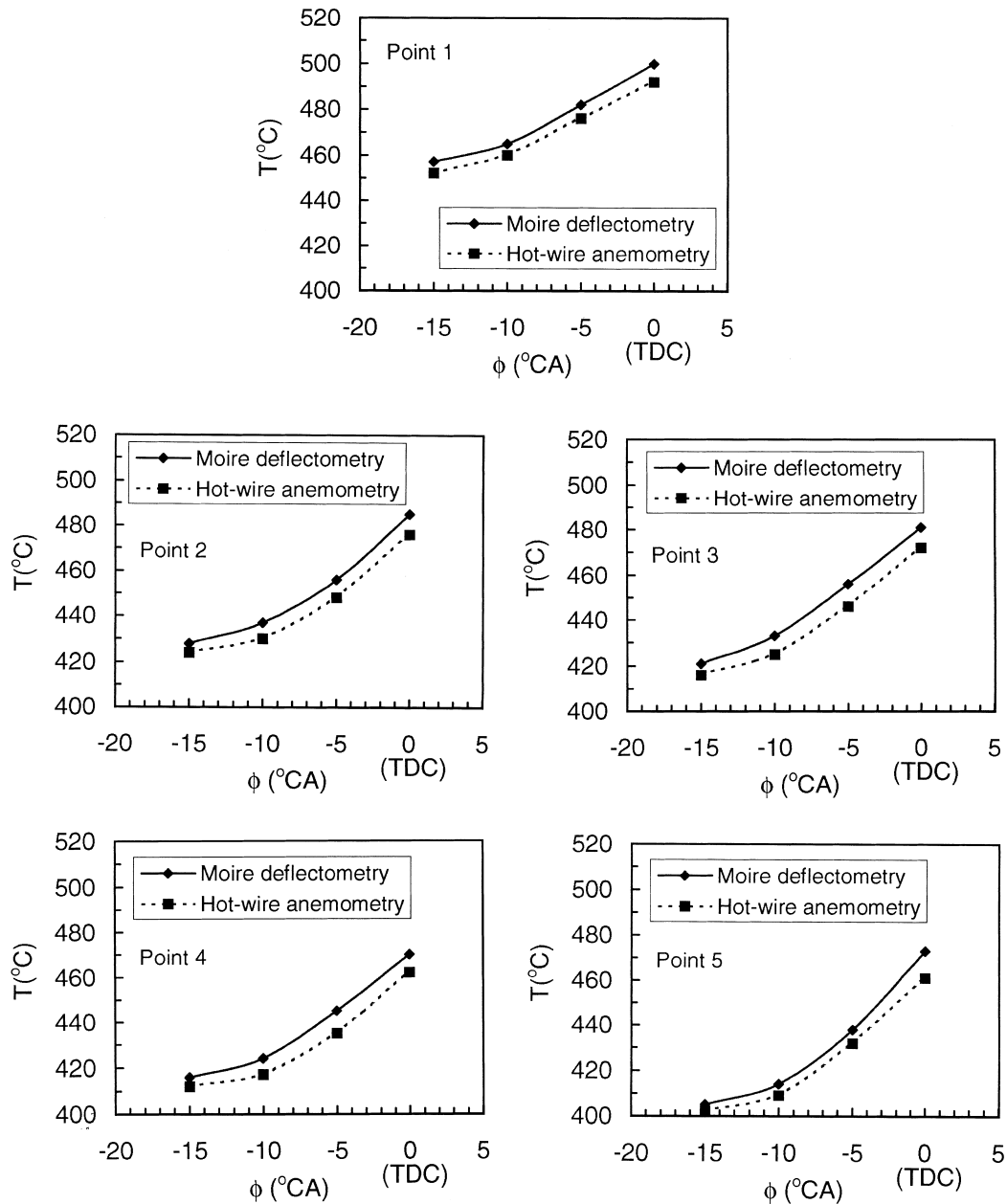


Fig. 9. Comparison of temperatures measured by Moire deflectometry and hot-wire anemometry.

The discrepancies increase slightly as the temperature is getting higher. Considering the effects of the thermal inertia of the hot-wire probe and the radiative heat exchange between the probe and the surroundings, the temperature distribution obtained by Moire deflectometry are remarkable.

## 6. Conclusions

Moire deflectometry has been successfully used to measure the transient temperature distribution in the swirl chamber of an IDI engine. The technique has great promise for the temperature measurement in confined combustion chamber of IC engines for its advantages of field measurement, fast response and non-disruption. The method to determine the temperature distribution from the detected Moire fringes is established. It is suggested that the transient wall surface temperature of the swirl chamber can be used as the reference point in the Moire fringe mapping. Measured temperatures in the swirl chamber are validated using hot-wire anemometry at the different positions, and the results are satisfactory.

The temperatures measured in the experiment provide useful information for the analysis of the fuel evaporation and mixing process in the swirl chamber during compression stroke. The engine performance could be improved by optimizing the design of the combustion system.

## Acknowledgements

We are grateful to the National Science Foundation of China for their support in this research work, and to Professor Yan Dapeng and Professor He Anzi of Nanjing University of Science & Technology for their helpful instruction.

## References

- [1] D.T. Li, Study and Design on the Swirl Chamber of IDI Engine. Machinery Industry Press, Beijing (in Chinese), 1986.
- [2] C.M. Vest, Interferometry of strong refracting axisymmetric phase object, *Appl. Opt.* 14 (7) (1975) 1601–1606.
- [3] O. Kafri, Moire deflectometry: a ray deflection approach to optical testing, *Optics Letters* 5 (12) (1980) 444–460.
- [4] E. Keren, Measurements of temperature distribution of flame by Moire deflectometry, *Appl. Opt.* 20 (12) (1981) 4263–4266.
- [5] J. Stricker, Analysis of 3-D phase object by Moire deflectometry, *Appl. Opt.* 23 (1984) 3657–3659.
- [6] A. Almasreh, M.A.G. Abushagur. Moire deflectometry in aero-optics analysis. Proceedings of the IEEE Southeastcon'92, 1992, pp. 570–572. Birmingham, U.S.A.
- [7] G. Toker, D. Levin, J. Stricker, Experimental investigation of supersonic/hypersonic flow fields based on a new approach using holographic optical techniques, in: Proceeding of the 16th IEEE International Congress on Instrumentation in Aerospace Simulation Facilities, Dayton, U.S.A., 1995, pp. 10.1–10.7.
- [8] E. Bar-Ziv, S. Sgulim, O. Kafri, E. Keren, Temperature mapping in flames by Moire deflectometry, *Appl. Opt.* 22 (5) (1983) 698–705.

- [9] W.Y. Lian, The structure and internal properties of underexpanded exhaust jets. International Symposium on Refined Flow Modeling and Turbulence Measurements. Iowa, U.S.A., 1985, pp. 53–57.
- [10] J.D. Trolinger, Holography for Aerodynamics, *Astronautics Aeronautics* 10 (8) (1982) 56–61.